Macromolecules

Article

Cite This: Macromolecules 2018, 51, 4220−4228

High Refractive Index Polymers by Design

Thorben Badur,[†] Christian Dams,[†] and Norbert Hampp*[,†,‡]

[†]Department of Chemistry and [‡]Material Science Center, Philipps University Marburg, Hans-Meerwein-Str. 4, 35032 Marburg, Germany

Supporting Information

ABSTRACT: We show that key parameters of high refractive index (HRI) polymers may be accurately predicted based on the data of the HRI group and the polymer backbone comprising the spacer (S) and polymerizable group (PG). Five different HRI groups and the corresponding siloxane and methacrylate homopolymers were considered in this work. As a testbed we have chosen HRI polymers for ophthalmological implants, e.g., intraocular lenses, defining the figures-of-merit. In this case they need to be nonabsorbing throughout the visual wavelength range and should have a high refractive index n_D and a high Abbe number ν_A as well. Finally, a low glass transition temperature T_g is required to receive flexible materials. All ten HRI polymers, among them five prepared first within this study, were synthesized and characterized. The received properties match the predicted within percentage range and show that the straightforward design principles introduced here are highly productive tools for polymer design.

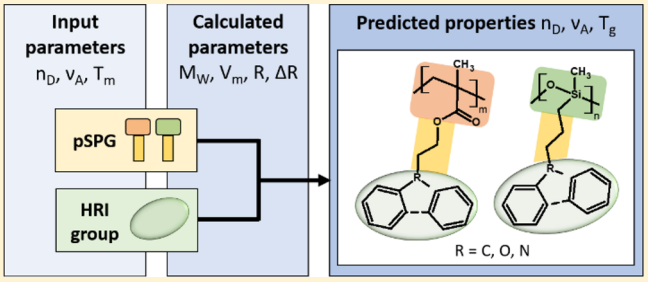

1. INTRODUCTION

Polysiloxanes (pSX) and polymethacrylates (pMA) are widely used in medicine, in particular as ophthalmic implants, e.g., as intraocular lenses (IOLs). Implantation of polymeric IOLs is the method of choice for the treatment of cataracts, the irreversible blurring of the human eye lens caused by protein misfolding and aggregation.[1,2] Because these polymers stay in the body for decades, their biocompatibility is essential. The state-of-the-art implantation technique is microincision cataract surgery (MICS).[3,4] The IOL needs to be folded and then is administered via a shooter into the capsular bag. For that reason the polymer requires a sufficient degree of flexibility at room temperature, meaning that the glass transition point T_g should be well below room temperature. For the optical properties of the IOLs a high refractive index n_D and a high Abbe number ν are desired to enable thin lenses and sharp images. Of course, an excellent transparency throughout the visual wavelength range is mandatory. Polysiloxanes and polymethacrylates fulfill these requirements. Two classes of polymers are in use today, termed as hydrophobic and hydrophilic. Each class has its specific pros and cons.

The first silicone-based IOL was implanted in a human eye by Zhou in 1978.[5] Poly(dimethylsiloxane) (pDMS) and poly(dimethylsiloxane-*co*-diphenylsiloxane) (pDMDPS) are mainly used as lens materials. The have refractive indices ranging from n_D = 1.41−1.46.[6] The incision required for the shooter is relatively large, ϕ = 3.2 mm and higher; because of the relatively low refractive index, the IOLs are rather thick lenses. Hydrophobic acrylic IOLs, on the other hand, possess refractive indices between 1.44 and 1.55, enabling incisions of ϕ < 2.2 mm.[7] To allow even smaller incisions, higher refractive indices n_D are required. Polymers with n_D values higher than 1.55 (n_D > 1.55) are called high refractive index (HRI) materials.

The design of polymers is often in a trial-and-error approach. We postulate that the optical properties of such a HRI polymer are dominated by the optical properties of the HRI group, in particular refractive index and Abbe number. The Abbe number defines the dispersion of the polymer and should be beyond 30 (ν_{Abbe} > 30) for IOLs to avoid chromatic aberration.[8] The relation between refractive index and the Abbe number is antiproportional.[9] HRI polymers are used in many areas, among them the optoelectronics field.[10] Structures commonly used are carbazole, stilbene, fluorene, and biphenyl derivatives.[11−13] In many applications high glass transition temperatures (T_g) are acceptable or even desired, but in the ophthalmology field T_g values far below the body temperature and even below room temperature are required (T_g < 18 °C). The T_g of a polymer is affected by many parameters, among them π-stacking of the side-chains, the free volume in the polymer, and others.

Chemically speaking, typical HRI polymers comprise a high refractive index group (HRI), a flexible spacer (S), and a polymerizable group (PG) (Figure 1). We show that the properties of such polymers may be designed from scratch starting with the HRI group and the polymerized polymer backbone (pSPG). The properties of the polymers may be predicted with good precision following the sketch given in Figure 2.

Received: March 22, 2018
Revised: May 9, 2018
Published: May 24, 2018

DOI: 10.1021/acs.macromol.8b00615
Macromolecules 2018, 51, 4220−4228

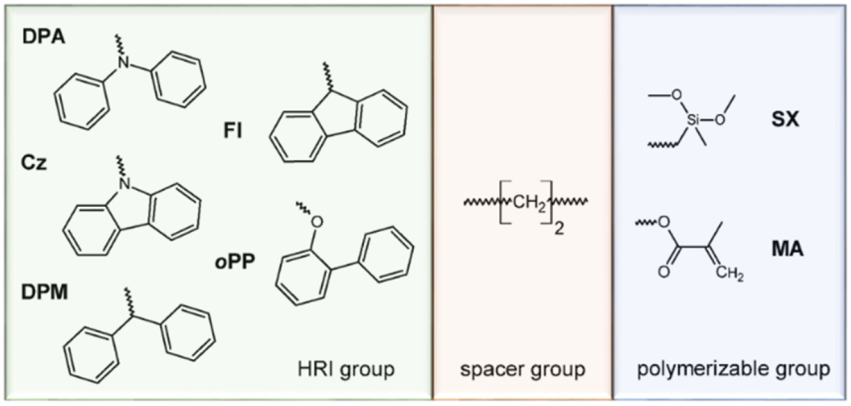

Figure 1. Overview of the building blocks of the examined acrylate and siloxane monomers. HRI groups (left), spacer group (middle), and polymerizable groups (right).

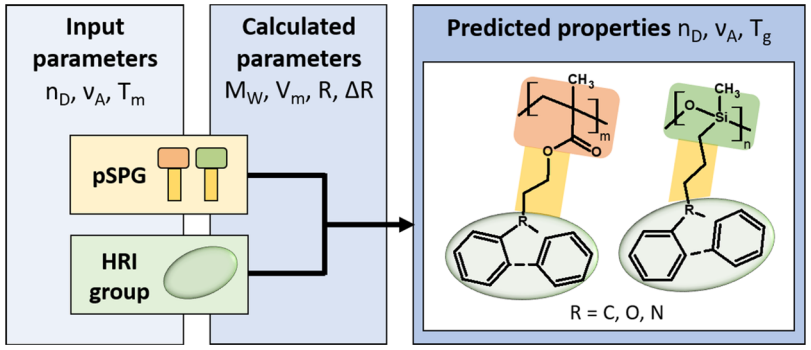

Figure 2. Model for the mathematical prediction of refractive index, Abbe number, and glass transition temperature of polymers.

Scheme 1. Structures of the Synthesized HRI-Polysiloxanes (Upper Row) and the Corresponding HRI-Polymethacrylates (Lower Row)[a]

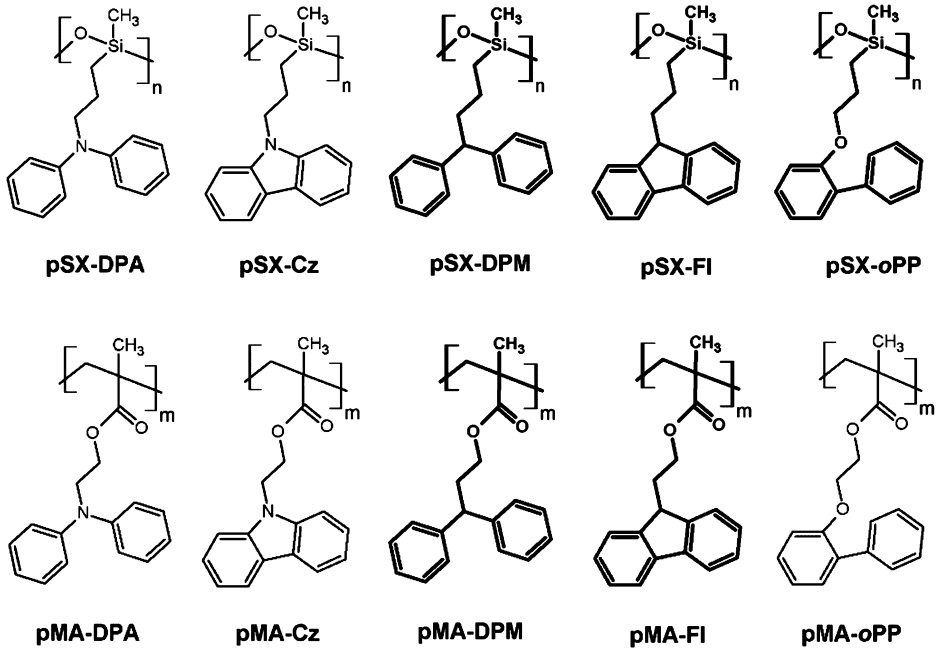

[a]Those synthesized first here are given in bold.

To test the proposed time-saving design tool for functional polymers for optical applications (here tested for HRI polymers for IOLs), we calculated the monomer and polymer properties for a set of 10 polymers, among them five novel polymers, and found that the theoretical predictions correlate very nicely with the experimental values obtained.

Throughout this study the spacer group was kept constant, i.e., an ethylene unit. Carbazole (Cz) was chosen as starting

DOI: 10.1021/acs.macromol.8b00615
Macromolecules 2018, 51, 4220−4228

Table 1. Refractive Indices of the HRI Groups Investigated[a]

		HRI group					SPG type	
		DPA	Cz	DPM	Fl	*o*PP	SPG_{SX}	SPG_{MA}
molar weight (M)	g/mol	169.23	167.21	168.24	166.22	170.21	148.28	114.14
melting point (T_m)	°C	53[26]	244[27]	25[28]	115[29]	59[30]	−115	−75
density (ρ)	g/cm^2	1.088	1.229	0.996	1.120	1.111	0.842	0.906
mol vol (V_m)	cm^3/mol	155.4	135.9	168.8	148.3	153.1	176.0	125.9
mol refraction (R)	cm^3/mol	55.62	56.37	55.56	53.79	52.72	42.05	31.18
refract index ($n_{D,calc}$)		1.634	1.767	1.572	1.645	1.604	1.393	1.409
refract index ($n_{D,20}$)		1.636[b]	1.708[c]	1.578	1.640[b]	1.610[b]	1.394	1.414
color		clear	beige	clear	clear	clear	clear	clear

[a]All values given in rows 3−6 were calculated using ACD/Laboratories. [b]Determined via extrapolation of serial dilution measurements in toluene. [c]Determined via extrapolation of serial dilution measurements in 1-ethyl-3-methylimidazolium methanesulfonate.

point for the HRI group as it is well-known in the literature in polysiloxanes and also for its high refractive index.[14] Novel siloxane polymers, based on carbazole, have been developed and successfully tested for application as IOLs lately with excellent biocompatibility.[15,16] Materials based on carbazole are usually colored and show high glass transition temperatures, which is as mentioned above, less desired for IOL polymers. For this reason, related structures with two aromatic benzene rings were selected, which should provide better performance for this parameter. Diphenylamine (DPA) has a similar electronic structure but provides two flexible unlinked aromatic rings, which should lead to lower glass transition temperatures. The corresponding aliphatic derivatives diphenylmethane (DPM) and fluorene (Fl) were included in this study because of their reduced polarity due to the heteroatom exchange. To see which influence comes from the structural characteristics of the HRI unit (branched vs linear), we included *o*-phenylphenol (*o*PP). The siloxane and methacrylate polymers synthesized are shown in Scheme 1.

2. EXPERIMENTAL SECTION

The five HRI groups were reacted to their siloxane and methacrylate precursors in preparation of the following monomer synthesis. The syntheses were carried out analogously, starting each with the corresponding HRI main component. The reaction conditions and bases were adjusted to the acidity of each component. After deprotonation with a base, the nucleophilic substitution of 2-chloroethanol or 2-bromoethanol leads to the desired methacrylate HRI-spacer precursor while a reaction with allyl bromide forms the siloxane precursor. Five HRI-allyl derivatives were synthesized in preparation for the siloxanes and five HRI-ethan-1-ol derivatives for the methacrylates.

Following, the precursors were converted to the respective monomers. For the allyl precursor systems a hydrosilylation was executed with dimethoxy(methyl)silane in the presence of Pt(0). The couplings were realized using a Karstedt's catalyst (platinum(0)-1,3-divinyl-1,1,3,3-tetramethyldisiloxane), analogously to a synthesis described earlier.[17,18] Starting from the prepared ethyl alcohol species, the nucleophilic substitution of methacryloyl chloride was performed in dichloromethane in the presence of triethylamine as auxiliary base.

In the next step polymers were prepared from the monomers and characterized. The polymerization of the siloxanes was performed, using sulfuric acid to start polycondensation. The received polymer samples went through a post-treatment *in vacuo* at higher temperatures to minimize monomer residuals. We reproduced the earlier reported polysiloxane based on carbazole (pSX-Cz) but synthesized and characterized also the partially described diphenylamine-substituted derivative (pSX-DPA).[19] In addition, three novel polymers were prepared based on diphenylmethane (pSX-DPM), fluorene (pSX-Fl), and *o*-phenylphenol (pSX-*o*PP) (Scheme 1, upper row). The progress of the polycondensation was monitored via FT-IR spectroscopy and weighing of the samples in order to determine the amount of methanol released during conversion. In case of complete polycondensation and subsequent thermal curing of the material, no methanol residues or remaining methoxy groups are present in the material. The peak of the $-O-CH_3$ valence vibration at a wavenumber of 2820 cm^{-1} (literature: 2850−2810 cm^{-1})[20] completely disappears during polymerization.

The methacrylate monomers were polymerized using a photochemically started radical polymerization. The methacrylates based on *o*-phenylphenol (pMA-*o*PP) and carbazole (pMA-Cz) are in technical use. In addition to this, the HRI-methacrylates based on diphenylamine (pMA-DPA) and the novel derivatives based on diphenylmethane (pSX-DPM) and fluorene (pSX-Fl) were prepared (Scheme 1, lower row). A post-treatment was also performed for the methacrylate homopolymers. The samples were repeatedly soaked in acetonitrile, and the solvent was analyzed via HPLC chromatography. Finally, it was removed completely at 80 °C. The polymers were analyzed by IR spectroscopy and HPLC analysis. Absence of the IR absorption band at 1630−1640 cm^{-1} indicates the absence of residual monomer. All details of syntheses and analyses of the polymers are given in Supporting Information 1.

3. RESULTS AND DISCUSSION

We start with the treatment of the refractive index and then study the Abbe number and finally the glass transition temperature. Because these polymers are designed for an application as a polymeric lens, we discuss also the relation between Abbe number and Sellmeier's formula.

3.1. Refractive Indices of the HRI Unit and SPG.

Starting from the structural formula of each HRI group, its molecular weight M is obtained. The density ρ is calculated with a modeling program, in this case ACD/Laboratories,[21] using tabulated additive atomic increments. The molar volume V_m is then derived using eq 1

$$V_m = M/\rho \tag{1}$$

where M is the molecular weight and ρ the density of the molecule. Molar refractions R are calculated by adding up atomic incremental values.[22,23] Finally, the refractive indices for the HRI groups are calculated using the Lorentz−Lorenz equation (eq 2)[24,25]

$$n_D = \pm\sqrt{\frac{1 + 2R/V_m}{1 - R/V_m}} \tag{2}$$

where R is the molar refraction and n_D is the refractive index at 589 nm. The second part of the molecules comprises the spacer and one of the polymerizable groups (SPG). The procedure is the same as for the HRI group. From tabulated incremental values the density, molar volume, and refractive index are

DOI: 10.1021/acs.macromol.8b00615
Macromolecules 2018, 51, 4220−4228

computed. The values calculated as well as the measured refractive indices are summarized in Table 1.

The siloxane spacer structure seems to be less attractive as it has a lower refractive index and a noticeably higher molecular weight. However, the molar weights of both units are rather similar after polymerization due to the different polymerization reactions, radical addition versus polycondensation. The molar weight of the effective repetitive unit is M = 114.14 g/mol for the methacrylates and M = 102.21 g/mol for the siloxanes.

3.2. Refractive Indices of the Monomers. A direct calculation of the refractive indices of the HRI-monomers is theoretically possible, but the results obtained were not satisfactory (see Supporting Information 2). We followed an alternative route. An aliphatic spacer, like the one used in our experiments, has no significant electronic influence on the aromatic HRI unit. Thus, we calculate the optical properties of the monomers from the HRI group and the SPG unit, assuming that each unit is contributing proportionally to the monomer. The refractive indices of the monomers n_D were obtained from a linear combination of the refractive indices of both structural units. The molar weight fractions of the HRI group in the monomer, given by the factor p, and the SPG group, given by $1 - p$, add up to the refractive index n_D of the monomer. The monomers differ from their building blocks by the loss of the terminal bonds of the HRI group (R′−H) and the SPG group (C−H) and the formation of a new R′−C bond in both cases (see Scheme 2). This is represented by the correction term

Scheme 2. Sketch of the Reaction of the HRI Groups with the Acrylate and Siloxane Based Linkers

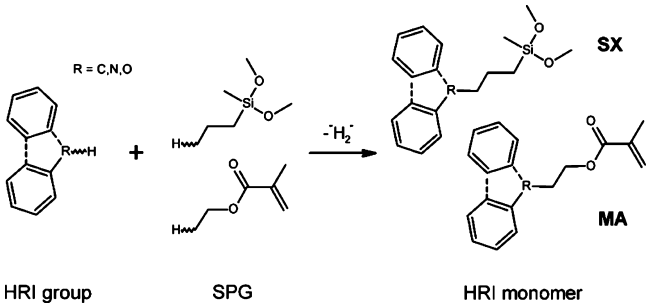

$n_{R'-C}$ which, is 0.039 for methacrylates as well as siloxanes (see Supporting Information 3). The refractive indices of the monomers $n_{D,WT\%}$ are computed using eq 3

$$n_{D,WT\%} = pn_{HRI} + (1 - p)n_{SPG} + n_{R,-C} \quad (3)$$

where p is the molar weight proportion of the HRI group from the monomer, n_{HRI} the refractive index of the HRI unit, n_{SPG} the refractive index of the attached spacer with polymerizable group, and $n_{R'-C}$ the correction term used. In Table 2 the calculated and measured refractive indices are shown. The excellent correlation between the calculated values using our "building block addition" method and the experimentally obtained values is obvious (Figure 3). Most of the theoretical values are slightly higher than the experimental ones. This may be due to minor impurities in the monomers from the syntheses.

3.3. Refractive Indices of the Polymers. The refractive indices n_D of the polymers are expected to be higher than those of the monomers due to the more dense packing (polymerization shrinkage). We model this process starting from the refractive index of the polymerized SPG groups and then attach the HRI group to the ready-made polymer backbone (eq 3).

The siloxane and methacrylate polymer backbones, comprising polymerizable group and the aliphatic spacers (ethyl methacrylate or dimethoxy(dimethyl)siloxane), were polymerized. After completion of the post-treatment, the physical properties of the polymerized SPGs (pSPG-MA and pSPG-SX) were determined (Table 3).

The refractive indices of the different polysiloxanes and the polymethacrylates were derived using the same model than applied for the monomers. The experimentally obtained refractive indices of the polymerized backbones were used. The refractive indices of the HRI groups and the polymerized

Table 2. Refractive Indices of the Monomers, Calculated and Experimentally Determined

monomer		p = WT %$_{HRI}$	$n_{D,exp}$	$n_{D,WT\%}$	$\Delta n_{D,WT\%}$	
SX	SX-DPA	53%	1.556	1.562	+0.006	+0.4%
	SX-Cz	53%	1.587	1.599	+0.012	+0.8%
	SX-DPM	53%	1.529	1.531	+0.002	+0.1%
	SX-Fl	53%	1.562	1.563	+0.001	+0.1%
	SX-*o*PP	53%	1.541	1.548	+0.007	+0.5%
MA	MA-DPA	60%	1.577	1.586	+0.009	+0.6%
	MA-Cz	60%	1.627[a]	1.629	+0.002	+0.1%
	MA-DPM	60%	1.552	1.551	−0.001	−0.1%
	MA-Fl	59%	1.589	1.588	−0.001	−0.1%
	MA-*o*PP	60%	1.572	1.570	+0.002	+0.1%

[a]Determined via extrapolation of measured values taken around melting temperature.The experimentally obtained values are marked as $n_{D,exp.}$ and the calculated ones as $n_{D,WT\%}$.

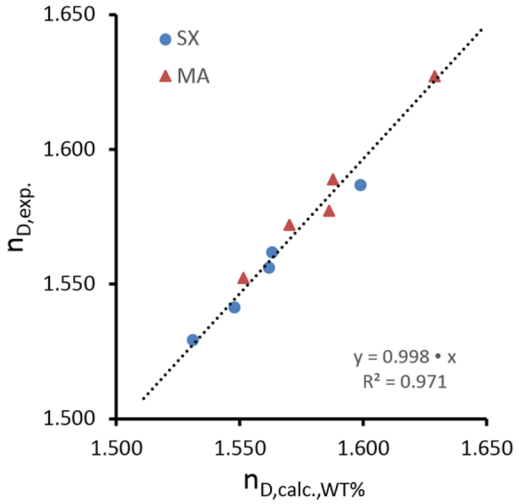

Figure 3. Comparison of the calculated and experimental values for n_D of all monomers. (blue dots = siloxanes, red triangles = methacrylates).

Table 3. Refractive Index and Abbe Number of the Polymerized Siloxane and Methacrylate Monomer with the Aliphatic Spacer Attached[a]

polymer	pSX-SPG	pMA-SPG
refract. index ($n_{D,calc}$)	1.442	1.478
refract. index ($n_{D,20}$)	1.433	1.483
color	colorless	colorless

[a]All values given in row 1 were calculated using ACD/Laboratories.

DOI: 10.1021/acs.macromol.8b00615
Macromolecules 2018, 51, 4220−4228

backbones pSPG were combined weighted by their mass contribution. Because in the polycondensation reaction of the siloxanes there is some mass loss, the values for p = WT% get higher than for the monomers. As correction term for the binding of the HRI groups, the same factor $n_{R'-C}$ = 0.039 is applied as used for the monomers (eq 3), using n_{pSPG} instead of n_{SPG} (see Supporting Information 3). The calculated values for the refractive indices of the polymers are listed (Table 4) and compared with the experimentally obtained ones.

Table 4. Calculated and Experimental Refractive Indices of Siloxane and Methacrylate Polymers[a]

polymer		p = WT%$_{HRI}$	$n_{D,exp}$	$n_{D,WT\%}$	$\Delta n_{D,WT\%}$	
pSX	pSX-DPA	62%	1.599	1.602	+0.003	+0.2%
	pSX-Cz	62%	1.635	1.646	+0.011	+0.7%
	pSX-DPM	62%	1.567	1.566	−0.001	−0.1%
	pSX-Fl	62%	1.608	1.604	−0.004	−0.2%
	pSX-*o*PP	63%	1.578	1.586	+0.008	+0.5%
pMA	pMA-DPA	60%	1.614[b]	1.614	+0.000	+0.0%
	pMA-Cz	60%	1.645[c]	1.657	+0.012	+0.7%
	pMA-DPM	60%	1.588[b]	1.579	−0.009	−0.6%
	pMA-Fl	59%	1.631[c]	1.616	−0.015	−0.9%
	pMA-*o*PP	60%	1.607[b]	1.599	+0.008	+0.5%

[a]The experimentally obtained values are marked as $n_{D,exp}$ and the calculated as $n_{D,WT\%}$. [b]Determined via extrapolation of values taken below glass transition temperature. [c]Determined using diiodomethane as contact agent.

The $\pi-\pi$ interactions in the polymers are hard to predict by theoretical models. It should be mentioned that in this case, around our starting temperature of the measurements, all but one polymer are in the glassy state and rather flexible. This means that the $\pi-\pi$ interactions are not dominating. In view of the simplicity of the model, the theoretical results nicely agree with the experimental findings (see Figure 4).

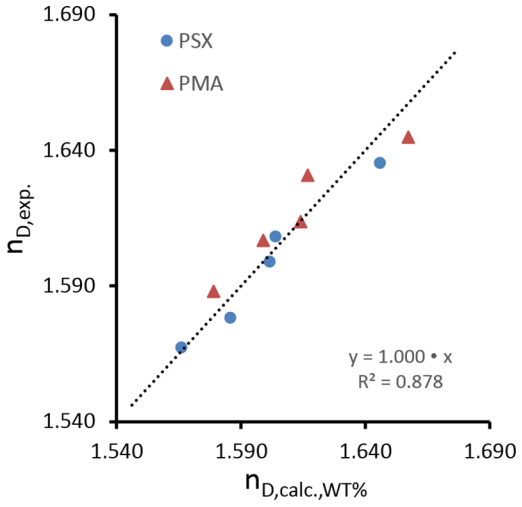

Figure 4. Correlation of the calculated and the experimentally obtained values for n_D for the examined polymers (blue dots = siloxanes, red triangles = methacrylates).

3.4. Abbe Numbers of the Polymers. Besides the refractive index of a polymer, the Abbe number ν is another important parameter for optical applications. It is a value which characterizes the optical dispersion ΔR of a material, i.e., the wavelength dependence of the refractive index $n(\lambda)$. The molar dispersion ΔR of the HRI groups as well as of the SPG group may be calculated similar to the refractive indices from tabulated values.[22,23] However, the errors using the calculated values for ΔR were too high. For that reason we used the experimentally obtained Abbe numbers ν_{exp} of the HRI groups, which are a side product of the wavelength-dependent refractive index measurements of the HRI groups, and calculated their molar dispersion ΔR via eq 4

$$\Delta R = \frac{6n_D}{(n_D^2 + 2)(n_D + 1)} \frac{R}{\nu_{exp}} \quad (4)$$

where ν_{exp} is the experimentally obtained Abbe number and n_D and R are as defined above. The respective values for each HRI group are summarized in Table 5.

The acrylates were polymerized radically, resulting in the loss of a double bond for the monomeric structure. The siloxanes were processed via polycondensation, resulting in the formal loss of one unit Me−O−Me for each monomer (see Scheme 3). The prepared polymers with attached spacer unit (pSPG) were characterized regarding their refractive index and Abbe number (Table 5), leading to calculated values for their mol. dispersion ΔR.

These molecular changes during polymerization lead to the correction term R_{poly} for the molar refraction, particularly R_{pMA} = −1.733 in the case of the polymethacrylates and R_{pSX} = −13.079 in the case of the polysiloxanes (details in Supporting Information 4). For attachment of the HRI group, different correction terms for every aromatic unit were applied due to the individual changes in polarizability and dispersion. These terms are marked as $R_{R'-C}$ (R′ = C, N, O) and $\Delta R_{R'-C}$ (see Supporting Information 5 for details). These correction factors allow the calculation of the Abbe numbers of the polymers $\nu_{polymer}$ following eq 5

$$\nu_{polymer} = \frac{6n_{D,calc}(R_{HRI} + R_{pSPG} + R_{R'-C})}{(n_{D,calc}^2 + 2)(n_{D,calc} + 1)(\Delta R_{HRI} + \Delta R_{pSPG} + \Delta R_{R'-C})} \quad (5)$$

where $n_{D,calc}$ are the calculated refractive indices based on our WT% model (see Table 4). R_{HRI} and R_{pSPG} are the molar refractions of the HRI and pSPG group, and $R_{R'-C}$ is the correction term for the formation of an R′−C bond. ΔR_{HRI} and ΔR_{pSPG} are the molar dispersions of both mentioned units while $\Delta R_{R'-C}$ is the correction term for the molar dispersion.

The Abbe numbers of the polysiloxanes and polymethacrylates are summarized in Table 6. Plotting the calculated Abbe numbers ν_A versus the experimentally obtained values shows a very good correlation between both (see Figure 5).

3.5. Glass Transition Temperatures. The melting temperature T_m of crystalline and semicrystalline polymers is considerably higher than that of the corresponding monomers. In case of cross-linked polymers, which do not possess a melting temperature, the glass transition temperature T_g is the relevant parameter which characterizes the temperature range where the polymer becomes flexible. We summarized the melting temperatures T_m of the HRI groups and of the spacer

DOI: 10.1021/acs.macromol.8b00615
Macromolecules 2018, 51, 4220−4228

Table 5. Experimentally Obtained Abbe Numbers and Dispersions of the HRI and SPG Groups[a]

		HRI					pSPG	
		DPA	Cz	DPM	Fl	*o*PP	pSX	pMA
abbe number (ν)		19.4[b]	17.3[c]	28.1	21.6[b]	23.1[b]	53.6	56.6
mol. refraction (R)	cm^3/mol	55.62	56.37	55.56	53.79	52.72	28.79	29.45
mol. refraction (ΔR)	cm^3/mol	2.28	2.51	1.62	1.97	1.83	0.47	0.44

[a]All values given in row 2 were calculated using ACD/Laboratories. [b]Determined via extrapolation of serial dilution measurements in toluene. [c]Determined via extrapolation of serial dilution measurements in 1-ethyl-3-methylimidazolium methanesulfonate.

Scheme 3. Sketch of the Two-Step Assembly of Acrylate (MA) and Siloxane (SX) Polymers[a]

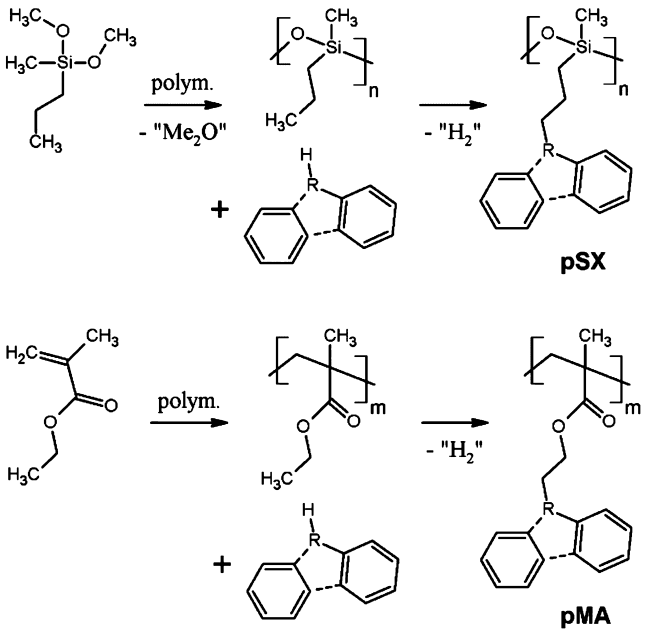

[a]In the first step just the backbone with spacers attached is considered, and in the second step the desired HRI group is attached schematically. The second step is identical to the theoretical treatment of the monomers.

Table 6. Calculated and Experimental Abbe Numbers of the Siloxane and Methacrylate Polymers

polymer		ν_{exp}	$\nu_{WT\%}$	$\Delta\nu_{WT\%}$	
pSX	pSX-DPA	23.1	23.9	+0.8	+3.5%
	pSX-Cz	20.3	21.9	+1.6	+7.9%
	pSX-DPM	32.7	33.1	+0.4	+1.2%
	pSX-Fl	24.6	26.9	+2.3	+9.3%
	pSX-*o*PP	27.7	28.5	+0.8	+2.9%
pMA	pMA-DPA	24.1[a]	24.2	+0.1	+0.4%
	pMA-Cz	21.5[b]	22.1	+0.7	+2.8%
	pMA-DPM	33.7[a]	33.5	−0.2	−0.6%
	pMA-Fl	25.7[b]	27.2	+1.5	+5.8%
	pMA-*o*PP	27.6[a]	28.9	+1.3	+4.7%

[a]Determined via extrapolation of values taken below glass transition temperature. [b]Determined using diiodomethane as contact agent.

polymerizable groups (SPG). The glass transition temperatures of the polymerized SPG (pSPG) were measured via DSC (Table 7).

In case of the glass transition temperature estimation, a number of models have been introduced based on the structure of the repeating unit.[31,32] These prediction models also widely use atomic additive contributions for the estimations.[33−35]

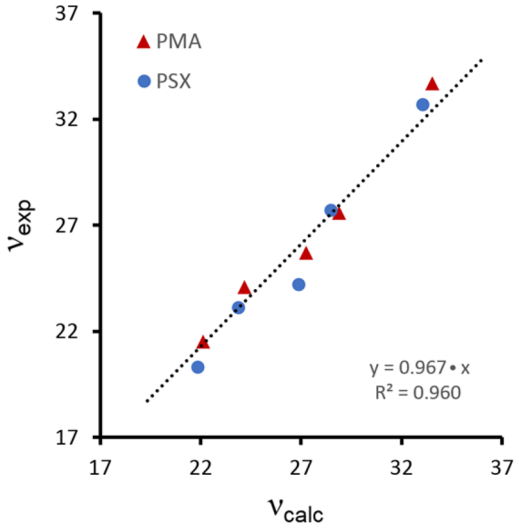

Figure 5. Comparison of the calculated and measured Abbe numbers for all synthesized siloxane (pSX) and methacrylate (pMA) polymers (blue dots = siloxanes, red triangles = methacrylates).

Table 7. Thermal Properties of the HRI Groups and SPGs/PSPGs Investigated

HRI group		DPA	Cz	DPM	Fl	*o*PP
melting point (T_m)	°C	53[26]	244[27]	25[28]	115[29]	59[30]
glass trans temp (T_g)	°C					
SPG/pSPG		SPG-SX	SPG-MA	pSPG-SX	pSPG-MA	
melting point (T_m)	°C	−115	−75			
glass trans temp (T_g)	°C			−122	62	

They nicely match with the experimental data, in particular for aliphatic polymers and such with aromatic units in their backbone, varying in their computational effort.[36,37] The calculation of T_g according to these models cannot deal with side chains increasing in size, length, complexity, and in particular with increasing interaction, e.g., π-stacking. The number of reliable atomic increments for heterocyclic structures is also limited.[33] Incorporation of a cross-linker further increases the complexity of the calculation. We were looking for a rather simple model, with focus on the high refractive groups, following our design model.

We follow again the same model introduced above for the refractive indices and Abbe numbers. The HRI group is schematically bound to one of the polymer backbones, i.e., pSPG-SX or pSPG-MA. The heat capacity of the resulting polymer is proportional to the number of bonds. To conclude from the melting and glass transition temperatures of the components to the glass transition temperature of the polymer, a proportionality factor S is introduced ($0 < S < 1$). The offset C compensates for the pure rise of the melting and glass

DOI: 10.1021/acs.macromol.8b00615
Macromolecules 2018, 51, 4220−4228

transition temperature due to the molecular weight increase (see eq 6).

$$T_{g,polymer} = (T_{m,HRI} + T_{g,pSPG})S + C \quad (6)$$

Using the data given in Table 7 and eq 6 the glass transition temperatures T_g of both polymer types can be derived. Slope and offset in combination define the properties of the HRI polymers. The values for the slope S and offset C were determined empirically to be $S_{SX} = 0.301$, $S_{MA} = 0.214$ and $C_{SX} = 121$ K, $C_{MA} = 200$ K. In Figure 6 the calculated values for the

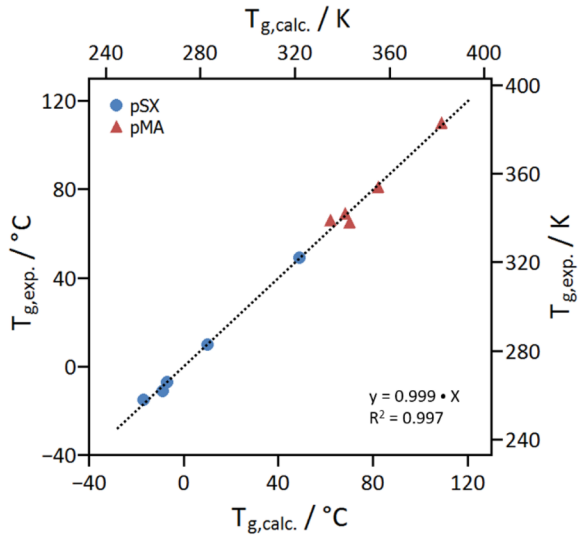

Figure 6. Comparison of the empirically determined method for deriving the glass transition temperature and the real value of the synthesized polymers.

T_g of the polymers are compared with the experimental data received (see Table 8). The DSC curves of all HRI polymers are shown in detail in Supporting Information 6.

Table 8. Thermal Properties of the Polymethacrylates and Polysiloxanes

polymer		pSX-DPA	pSX-Cz	pSX-DPM	pSX-Fl	pSX-*o*PP
exp glass trans temp ($T_{g,exp}$)	°C	−11	49	−15	10	−7
empirical calc glass trans temp ($T_{g,fit}$)	°C	−9	49	−17	10	−7
ΔT_g		−0.8%	+0.0%	+0.8%	+0.0%	+0.0%
polymer		pMA-DPA	pMA-Cz	pMA-DPM	pMA-Fl	pMA-*o*PP
exp glass trans temp ($T_{g,exp}$)	°C	69	110	66	81	65
empirical calc glass trans temp ($T_{g,fit}$)	°C	68	109	62	82	70
ΔT_g		+0.3%	+0.3%	+1.2%	−0.3%	−1.5%

3.6. Sellmeier Equation. For the design of high quality lenses, e.g. IOLs, it is useful to have a description for the optical dispersion. The sellmeier dispersion formula[38] is used in optics design to describe the relationship between the refractive index n^2 and the wavelength λ for transparent materials (eq 7)

$$n^2(\lambda) = A + B\frac{\lambda^2}{\lambda^2 - {\lambda_0}^2} \quad (7)$$

Here A ($A \geq 1$) is a parameter representing the contribution of the UV term. The dimensionless parameter B is defining the shape of the refractive index in the visible light spectrum. λ_0 (in nm) is the resonance wavelength of the absorbing molecule. As this equation is derived for glassy nonabsorbing materials, some deviations may occur for rigid, partially colored polymethacrylates. The flexible polysiloxanes, however, can be described very well using this method. The values calculated using a best-fit method for the five polymethacrylates and five polysiloxanes are summarized in Table 9.

Table 9. Determined Values for the Sellmeier Factors *A*, *B*, and λ_0

polymer		abbe number	*A*	*B*	λ_0
PSX	PSX-DPA	23.1	1.990	0.468	245.1
	PSX-Cz	20.3	2.121	0.424	268.2
	PSX-DPM	32.7	1.720	0.666	183.0
	PSX-Fl	24.6	2.000	0.484	242.0
	PSX-*o*PP	27.7	1.840	0.565	212.0
PMA	PMA-DPA	24.1[a]	2.140	0.369	252.0
	PMA-Cz	21.5[b]	1.970	0.612	238.0
	PMA-DPM	33.7[a]	1.460	0.983	158.0
	PMA-Fl	25.7[b]	1.990	0.525	230.0
	PMA-*o*PP	27.6[a]	1.880	0.616	208.0

[a]Determined via extrapolation of values taken below glass transition temperature. [b]Determined using diiodomethane as contact agent.

The Abbe numbers of the polymers are showing a clear correlation with the Sellmeier factor *B*, defining the shape of the dispersion curve. In case of the polymethacrylates, the rigid pMA-Cz, showing a glass transition temperature beyond 100 °C, was excluded from the fitting (given within parentheses) (Figure 7). Whereas *A* has only limited effect on the Abbe number, the *B* value directly correlates to the Abbe number. The higher the *B* value, the easier high Abbe numbers may be obtained. The respective dispersion curve of each polymer and their corresponding absorption graph are shown in Supporting Information 7.

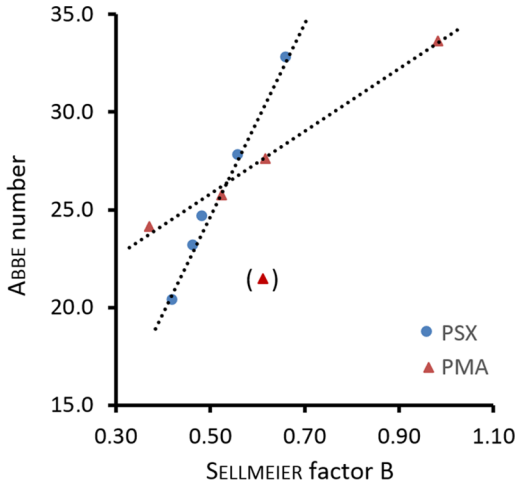

Figure 7. Relation between the Sellmeier factor *B* and the Abbe number.

DOI: 10.1021/acs.macromol.8b00615
Macromolecules 2018, 51, 4220−4228

Table 10. Comparison of Refractive Index, Abbe Number, and Glass Transition Temperature of the Investigated Polymers

properties		$n_{D,exp}$	$n_{D,WT\%}$	ν_{exp}	$\nu_{WT\%}$	$T_{g,exp}$	$T_{g,fit}$	blue wool scale
figure-of-merit		$n_D > 1.550$		$\nu > 30.0$		$T_g < 18$ °C		
pSX	pSX-DPA	**1.599**	**1.602**	23.1	22.9	**−11**	**−9**	2
	pSX-Cz	**1.635**	**1.646**	20.3	21.9	49	49	2[a]
	pSX-DPM	**1.567**	**1.566**	**32.7**	**33.1**	**−15**	**−17**	**4**
	pSX-Fl	**1.608**	**1.604**	24.6	26.9	**10**	**10**	4
	pSX-*o*PP	**1.578**	**1.586**	27.7	28.5	−7	−7	6
pMA	pMA-DPA	**1.614**	**1.614**	24.1	24.2	69	68	1
	pMA-Cz	**1.645**	**1.657**	21.5	22.1	110	109	3
	pMA-DPM	**1.588**	**1.579**	**33.7**	**33.5**	66	62	5
	pMA-Fl	**1.631**	**1.616**	25.7	27.2	81	82	4
	pMA-*o*PP	**1.607**	**1.599**	27.6	28.9	65	70	6

[a]Determined using the alternative pathway (see Supporting Information 8).

4. SUMMARY

We introduce a simple and effective approach to predict the optical and thermal parameters of polysiloxane and polymethacrylate polymers in their glassy state, speeding up the design process for such polymers significantly. The polymer parameters can be predicted from those of the HRI group and of the polymer backbone pSPG. In Table 10 the experimentally obtained and the numerically calculated values are summarized for all three parameters examined: the refractive index n_D, the Abbe number ν, and the glass transition temperature T_g.

To determine the influence of the reaction pathway, the polysiloxanes were also synthesized via an alternative route. The second route was performed using a hydrosilylation and prepolymerized pMHS and showed similar physical results like the polymers obtained via polycondensation reaction (details in Supporting Information 8).

Those values given in bold numbers match the figure-of-merit for the selected application, here polymers for intraocular lenses. In addition, the lightfastness of the examined homopolymers, without any UV-absorber added, are given in the rightmost column. Only one out of the set of 10 homopolymers studied matches all the desired criteria: pSX-DPM. All others reach the required high refractive index but fail in another parameter, in particular the Abbe number. The semiquantitative calculation tool introduced here may massively reduce and speed up lab work, in the example shown by 90%.

5. CONCLUSION

The design of polymers for a particular application, here for intraocular or contact lenses, leads to a set of parameters that need to be fulfilled in combination. Sequential optimization of the different parameters does not lead to the desired result. Computational methods that consider the interdependence of the different parameters, in this case the refractive index n_D, the Abbe number ν, and the glass transition temperature T_g, significantly ease the development and reduce lab work. The theoretical model introduced comprises a set of building blocks which combined provide a sufficiently precise prediction for the polymer properties, in our example novel highly flexible high refractive index optical polymers, as required for intraocular or contact lenses. We verified the theoretical concept introduced using a set of ten polymers, among them five novel polymers.

■ ASSOCIATED CONTENT

Supporting Information

The Supporting Information is available free of charge on the ACS Publications website at DOI: 10.1021/acs.macromol.8b00615.

(1) Monomer and polymer syntheses, (2) calculation of monomer refractive indices, (3) derivation of the correction term n_{R-C}, (4) refraction change during polymerization, (5) correction terms for HRI group attachment, (6) thermal properties of the HRI polymers, (7) optical properties and Sellmeier function, and (8) alternative pathway for pSX derivatives (PDF)

■ AUTHOR INFORMATION

Corresponding Author

*(N.H.) E-mail hampp@uni-marburg.de, phone +49 6421 2825775, fax +49 6421 2825798.

ORCID

Norbert Hampp: 0000-0003-1614-2698

Notes

The authors declare no competing financial interest.

■ ACKNOWLEDGMENTS

Financial support through grant FKZ 13GW0047C from the German Federal Ministry of Education and Research (BMBF) is gratefully acknowledged. The authors thank the technical staff in the laboratory and Joshua Stoll and Tobias Kranz for their scientific contributions during their lab courses.

■ REFERENCES

(1) Lindstrom, R. Thoughts on Cataract Surgery: 2015; https://www.reviewofophthalmology.com/article/thoughts-on-cataract-surgery-2015 (accessed March 2, 2017).

(2) Moreau, K. L.; King, J. A. Protein Misfolding and Aggregation in Cataract Disease and Prospects for Prevention. *Trends Mol. Med.* **2012**, *18* (5), 273−282.

(3) Hayashi, K.; Yoshida, M.; Hayashi, H. Postoperative Corneal Shape Changes: Microincision versus Small-Incision Coaxial Cataract Surgery. *J. Cataract Refractive Surg.* **2009**, *35* (2), 233−239.

(4) Dewey, S.; Beiko, G.; Braga-Mele, R.; Nixon, D. R.; Raviv, T.; Rosenthal, K. Microincisions in Cataract Surgery. *J. Cataract Refractive Surg.* **2014**, *40* (9), 1549−1557.

(5) Auffarth, G. U.; Apple, D. J. Zur Entwicklungsgeschichte Der Intraokularlinsen. *Ophthalmologe* **2001**, *98* (11), 1017−1031.

(6) Kohnen, T. The Variety of Foldable Intraocular Lens Materials. *J. Cataract Refractive Surg.* **1996**, *22* (2), 1255−1258.

DOI: 10.1021/acs.macromol.8b00615
Macromolecules 2018, 51, 4220−4228

(7) Bandello, F.; Güell, J. L. *Cataract - Overview*; ESASO: 2013; Vol. 3.
(8) Matsuda, T.; Funae, Y.; Yoshida, M.; Yamamoto, T.; Takaya, T. Optical Material of High Refractive Index Resin Composed of Sulfur-Containing Aliphatic and Alicyclic Methacrylates. *J. Appl. Polym. Sci.* **2000**, *76* (1), 45−49.
(9) Zhao, H.; Mainster, M. A. The Effect of Chromatic Dispersion on Pseudophakic Optical Performance. *Br. J. Ophthalmol.* **2007**, *91* (9), 1225−1229.
(10) Higashihara, T.; Ueda, M. Recent Progress in High Refractive Index Polymers. *Macromolecules* **2015**, *48* (7), 1915−1929.
(11) McGrath, J. E.; Rasmussen, L.; Shultz, A. R.; Shobha, H. K.; Sankarapandian, M.; Glass, T.; Long, T. E.; Pasquale, A. J. Novel Carbazole Phenoxy-Based Methacrylates to Produce High-Refractive Index Polymers. *Polymer* **2006**, *47* (11), 4042−4057.
(12) Sun, J.; Cheng, J.-G.; Zhu, W.-Q.; Ren, S.-J.; Zhong, H.-L.; Zeng, D.-L.; Du, J.-P.; Xu, E.-J.; Liu, Y.-C.; Fang, Q. An X-Shaped p-Conjugated Polymer Comprising of Fluorene Units and Anthracene Units with High Efficiency. Synthesis and Optical and Electrochemical Properties. *J. Polym. Sci., Part A: Polym. Chem.* **2008**, *46*, 5616−5625.
(13) Gaudiana, R. A.; Minns, R. A. High Refractive Index Polymers. *J. Macromol. Sci., Chem.* **1991**, *28* (9), 831−842.
(14) Wang, T.; Ye, H.; Zhang, X.; Cheng, J. UV-Curable Epoxy Silicone with a High Refractive Index and Self-Photosensitizing Effect. *Ind. Eng. Chem. Res.* **2012**, *51* (49), 15832−15838.
(15) Xu, J.; Zhu, W.; Jiang, L.; Xu, J.; Zhang, Y.; Cui, Y. Carbazole-Grafted Silicone Hydrogel with a High Refractive Index for Intraocular Lens. *RSC Adv.* **2015**, *5*, 72736−72744.
(16) Xu, J.; Zhu, W.; Zhang, L.; Zhang, Y. Preparation and Characterization of Transparent and Foldable Polysiloxane-Poly-(Methyl Methacrylate) Membrane with a High Refractive Index. *J. Appl. Polym. Sci.* **2015**, *132* (36), 42491.
(17) Schraub, M.; Soll, S.; Hampp, N. High Refractive Index Coumarin-Based Photorefractive Polysiloxanes. *Eur. Polym. J.* **2013**, *49* (6), 1714−1721.
(18) Nordin, N. H.; Ramli, M. R.; Othman, N.; Ahmad, Z. Synthesis of Carbazole-Substituted Poly(Dimethylsiloxane) and Its Improved Refractive Index. *J. Appl. Polym. Sci.* **2014**, *132* (11), 41654.
(19) Belfield, K. D.; Chinna, C.; Najjar, O. Synthesis of Novel Polysiloxanes Containing Charge Transporting and Second-Order Nonlinear Optical Functionalities with Atom Economical Constructs. *Macromolecules* **1998**, *31* (9), 2918−2924.
(20) Coates, J. *Interpretation of Infrared Spectra, A Practical Approach*; John Wiley & Sons, Ltd.: Chichester, UK, 2006.
(21) Advanced Chemistry Development Inc. ACD/Physchem Profiler, ACD/Labs Percepta. 2016; p version 2016.2.
(22) Dean, J. A. *Lange's Handbook of Chemistry*, 15th ed.; McGraw-Hill: New York, 1999.
(23) Chemical Society of Japan. *Chemical Handbook Basic II*; Maruzen, Ed.; Maruzen: Tokyo, 1979.
(24) Lorenz, L. Ueber Die Refractionsconstante. *Ann. Phys.* **1880**, *247* (9), 70−103.
(25) Lorentz, H. A. Ueber Die Beziehung Zwischen Der Fortpflanzungsgeschwindigkeit Des Lichtes Und Der Körperdichte. *Ann. Phys.* **1880**, *245* (4), 641−665.
(26) Lide, D. R.; Milne, G. W. A. *Handbook of Data on Common Organic Compounds*; CRC Press: Boca Raton, FL, 1995; Vol. *I*.
(27) Creencia, E. C.; Horaguchi, T. Thermal Decomposition Reactions of N-Alkylated 2-Aminobiphenyls to Carbazole and Phenanthridine. *ChemInform* **2007**, *38*, 2−7.
(28) Serijan, K. T.; Wise, P. H. Dicyclic Hydrocarbons. III. Diphenyl- and Dicyclohexylalkanes through C15. *J. Am. Chem. Soc.* **1951**, *73*, 4766−4769.
(29) Mogalian, E.; Sepassi, K.; Myrdal, P. B. Accounting for the Effects of Moderately Increased Pressure on the Energetics of Melting and Solubility in Metered Dose Inhalers. *Drug Dev. Ind. Pharm.* **2008**, *34* (9), 930−935.
(30) Paulus, W. *Microbicides for the Protection of Materials: A Handbook*; Springer Science+Business Media: Dordrecht, 1993.
(31) Camelio, P.; Lazzeri, V.; Waegell, B.; Cypcar, C.; Mathias, L. J. Glass Transition Temperature Calculations for Styrene Derivatives Using the Energy, Volume, and Mass Model. *Macromolecules* **1998**, *31* (7), 2305−2311.
(32) Hopfinger, A. J.; Koehler, M. G.; Pearlstein, R. A.; Tripathy, S. K. Molecular Modeling of Polymers. IV. Estimation of Glass Transition Temperatures. *J. Polym. Sci., Part B: Polym. Phys.* **1988**, *26* (10), 2007−2028.
(33) van Krevelen, D. W.; te Nijenhuis, K. *Properties of Polymers*, 4th ed..; Elsevier B.V.: Amsterdam, 2009.
(34) Askadskii, A. A.; Matseevich, T. A.; Markov, V. A. Determination of Glass-Transition Temperatures of Polymers: A Modified Computational Scheme. *Polym. Sci., Ser. A* **2016**, *58* (4), 506−516.
(35) Bicerano, J. Prediction of the Properties of Polymers from Their Structures. *J. Macromol. Sci., Polym. Rev.* **1996**, *36* (1), 161−196.
(36) Mattioni, B. E.; Jurs, P. C. Prediction of Glass Transition Temperatures from Monomer and Repeat Unit Structure Using Computational Neural Networks. *J. Chem. Inf. Comput. Sci.* **2002**, *42* (2), 232−240.
(37) Keshavarz, M. H.; Esmaeilpour, K.; Taghizadeh, H. A New Approach for Assessment of Glass Transition Temperature of Acrylic and Methacrylic Polymers from Structure of Their Monomers without Using Any Computer Codes. *J. Therm. Anal. Calorim.* **2016**, *126* (3), 1787−1796.
(38) Sellmeier, W. Zur Erklärung Der Abnormen Farbenfolge Im Spectrum Einiger Substanzen. *Ann. Phys.* **1871**, *219* (6), 272−282.

DOI: 10.1021/acs.macromol.8b00615
Macromolecules 2018, 51, 4220−4228